Supramolecular chirality: a caveat in assigning the handedness of chiral aggregates

COMMUNICATION

Supramolecular chirality: A caveat in assigning the handedness of chiral aggregates

Received 00th January 20xx,
Accepted 00th January 20xx

DOI: 10.1039/x0xx00000x

K. Swathi,[a,b] Cristina Sissa,[a*] Anna Painelli [a] and K. George Thomas [b*]

The handedness of a supramolecular chiral aggregates is often assigned based on the sign of circular dichroism spectra, adopting the exciton chirality method. However, the method does not properly account for the nature of intermolecular interactions. We introduce a generalized picture on the use of the sign of chiral signals in determining the helicity of chiral aggregates, rooted in the exciton model, supported by TD-DFT results.

Chirality remains a fascinating area of research, encompassing all branches of science since the first observation of optical activity by François Arago in 1811.[1] Most of the initial research activities in the field were focused on molecular chirality with a significant impact on drug design. With the advent of supramolecular chemistry, the research activity in the area boosted, extending to macroscopic chirality and opening up promising applications in drug delivery,[2] catalysis,[3] nonlinear optics,[4] chiral sensing,[5] etc. The emergence of optical properties in supramolecular assemblies is governed by excitonic interactions. When two molecules are in close proximity, the electrostatic interaction between their transition dipole moments leads to the splitting of the excited state energy levels (exciton model).[6] As a typical example, in aligned dimers the exciton coupling leads to the emergence of new spectral features, specifically a blue-shifted absorption band compared to the monomer, denoted as H-band (H for hypsochromic) and a red-shifted absorption band for J-aggregate denoted as J-band (J for Jelly, one of the researchers who first observed J-aggregates).[6] In a classic work, Nakanishi and Harada brought out the implications of exciton coupling in chiral aggregates, providing the basis of the exciton chirality (EC) rule.[7] It states *"if the exciton circular dichroism (CD) shows a positive (negative) first and a second negative (positive) cotton effect, then the two electric transition dipole moments constitute a clockwise (anti-clockwise) screw sense"*.[7] Despite caution that the rule does not have a general validity, EC rule became the method of choice for chemists and biologists to experimentally determine the absolute handedness of chiral supramolecular and nanoscopic structures.[7, 8] Recently, a few exceptions to the EC rule were highlighted: they were ascribed to conformational disorder[9] or strong transition magnetic dipoles.[10] The exciton chirality rule for vibrational circular dichroism has been recently discussed to highlight its limitations and potentials.[11] Herein, we re-examine the EC rule for electronic circular dichroism, focusing on the relation between the sign of CD spectra and the absolute chirality of the supramolecular system. Moreover, we address the sum rule for CD spectra, underlying the limits of the exciton model. Results are supported by a detailed comparison with state of the art quantum chemical calculations.

To begin with, we considered a dimeric structure, built-up of equivalent molecules, as in Fig. 1. In the spirit of exciton

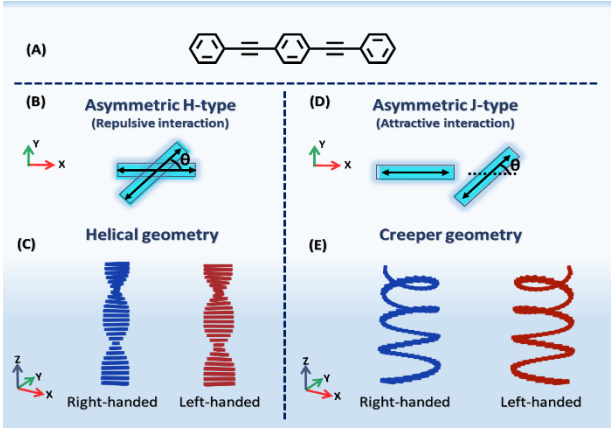

Figure 1 (A) Molecular structure of phenyleneethynylene (PE) used for creating helical and creeper geometries. PE possesses one transition dipole (TD) along its longitudinal axis, represented by a double-sided arrow. A top view of different chiral dimers with tilt angle θ (B,D) and a three dimensional sketch of larger aggregates (C,E). In all cases both right- and left-handed geometries are shown. (B,C) denote asymmetric H-type stacking with repulsive interactions and (D,E) denote asymmetric J-type stacking with attractive interactions.

[a] *Dipartimento di Scienze Chimiche, della Vita e della Sostenibilità Ambientale, Università di Parma, Parco Area delle Scienze 17/A, 43124, Parma, Italy.*
[b] *School of Chemistry, Indian Institute of Science Education and Research Thrivananthapuram (IISER-TVM), Trivandrum 695551, India*
[c] *Electronic Supplementary Information (ESI) available: [details of any supplementary information available should be included here]. See DOI: 10.1039/x0xx00000x*

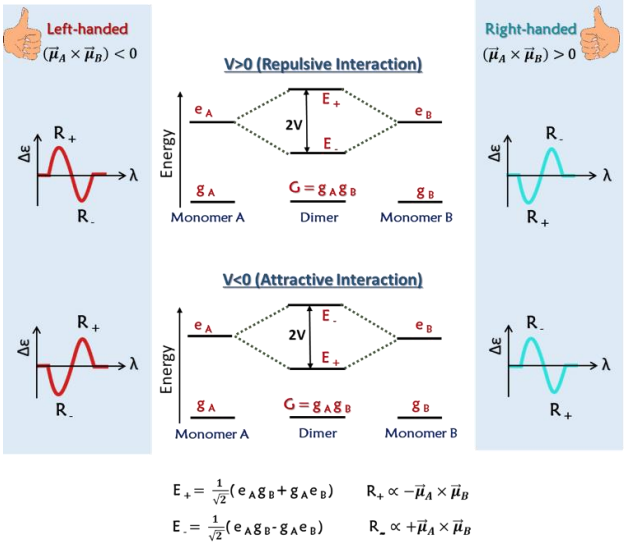

Figure 2 Schematic representation of the energy diagram for dimers with repulsive and attractive interactions using exciton model and corresponding bisignated circular dichroic (CD) spectrum for right- and left-handed dimers. The shaded left and right columns show the bisignated CD of the dimeric structures, organized in left- and right-handed fashion, respectively. The central column shows the energy level diagram for dimers with repulsive (V>0; top panel) and attractive (V<0; bottom panel) interactions.

model, each molecule is described in terms of just two electronic states: the ground ***g*** and the excited state ***e***, so that four states should be considered for a dimer: g_Ag_B, e_Ag_B, g_Ae_B, e_Ae_B, where A and B indices denote the two molecules. In the exciton model, only intermolecular interactions between the two degenerate states, e_Ag_B, g_Ae_B, are considered. As schematically shown in Fig. 2 (see also ESI), this leads to the in-phase (**E**$_+$) and out-of-phase (**E**$_-$) combination of the e_Ag_B and g_Ae_B states. The relative energy of the two states depends on the sign of the electrostatic interaction between the transition dipole moments on the two molecules, with the in-phase state lying lower (higher) in energy for the attractive (repulsive) interactions. The rotational strength associated with the two states reads:[8]

$$R_{\pm} = -\frac{\omega_{\pm}}{2}\,\vec{r}\cdot\left(\mu_{\pm}^{A}\times\mu_{\pm}^{B}\right), \qquad (1)$$

where ω± is the frequency of the $G \rightarrow E_{\pm}$ transition and $\mu_{\pm}^{A/B}$ is the contribution of the A/B molecules to the corresponding transition dipole moment. **R**$_+$ and **R**$_-$ have opposite sign, justifying the appearance of an exciton doublet (bisignation) whose sign changes for the left and right helical arrangements. The absolute sign of the doublet, however, depends on the relative energy of the **E**$_{+/-}$ states (see Fig. 2). For repulsive interactions (H-type), $\boldsymbol{E}_-$ is the lowest excited state so that the right-handed structure gives rise to a positive CD signal in the low-energy (higher wavelength) side of the doublet, in line with the exciton chirality rule.[7] However, the opposite occurs for attractive interactions (J-type) with **E**$_+$ lying lower than $\boldsymbol{E}_-$, so that for the right-handed structure a negative signal is expected in the low-energy side of the doublet, breaking the generality of exciton chirality rule.

The exciton model is very useful to understand the basic features of CD spectra. However, it suffers from a fundamental problem that is well evident from the above equation. A general and fundamental sum rule states that the sum of the rotational strengths for all the transitions must vanish.[12] In the exciton model, however, this rule is not obeyed: the geometrical part of the rotational strength (the term $\vec{r}\cdot\left(\mu_{\pm}^{A}\times\mu_{\pm}^{B}\right)$ in Equation 1) is indeed equal and opposite for the two transitions, but their (slightly) different frequencies lead to (slightly) different rotational strengths. As detailed in the ESI, this fundamental inconsistency is related to the approximation used in the exciton model and is solved by accounting for the intermolecular interactions that mix g_Ag_B, and e_Ae_B states.[13]

To validate our results, we compare CD spectra calculated in the exciton approximation with TD-DFT results. We select a linear phenyleneethynylene dye (**PE**, Fig. 1A), a rigid-rod like molecule characterized by a single low-lying excited state, as the molecular building block for the supramolecular structure.[14] The ground state geometry of the **PE** is optimized at the DFT level using the CAM-B3LYP functional and 6-31G(d) as basis set in the gas phase. The lowest energy transition is calculated at 313.13 nm with a transition dipole moment of 11.28 Debye, aligned along the main molecular axis. **PE** does not have a chiral centre but can be designed to form chiral supramolecular assemblies (Fig. 1). Specifically, we will consider two different supramolecular assemblies where **PE**s (frozen ground state geometry is calculated for the isolated dye) are arranged in a simple-helix (asymmetric H-type) and creeper-helix geometry (asymmetric J-type) as in Fig. 1C,E. Henceforth simple-helix and creeper-helix geometries are denoted as helix and creeper, respectively. In both geometries, twist angle between the monomers (θ, see Fig. 1B,D) is varied from 10° to 80° (at 0° and 90° the system is non-chiral and CD signals vanish). For the helix geometry, the intermolecular distance along z is fixed as 10 Å, maintaining the molecular centre at x=y=0. In the creeper geometry, the intermolecular distance along Z-axis is set to be 5 Å, and the molecular centre is displaced by 12 Å along X. In the helix, repulsive interactions among transition dipole moments make the $\boldsymbol{E}_-$ state lower in energy (Fig. 2). On the contrary, in the creeper, the X-displacement is large enough to guarantee attractive interactions and the **E**$_+$ state becomes the lower energy state.

Table 1 shows the transition energy, oscillator strength (f) and rotational strength (R) calculated using TD-DFT for helical and creeper dimers with various tilt angles. For small twist angles in the helix arrangement, the oscillator strength (roughly twice the oscillator strength of the monomer) is mainly concentrated in the high energy state, while the opposite occurs for the creeper dimer. This is in line with the exciton model for aligned molecules (θ=0°), which predicts that only a transition from the ground state to the **E**$_+$ state is allowed. Upon increasing θ, the oscillator strength redistributes between **E**$_+$ and $\boldsymbol{E}_-$ states. CD spectra in Fig. 3 and 4 are calculated assigning a Gaussian band shape to the two transitions (with standard deviation σ = 0.35 eV) using equation 2,[7, 15]

$$\Delta\varepsilon(\tilde{\nu}) = \sum_{i=1}^{n}\left(\frac{R_i\,\tilde{\nu}_i}{2.296\times10^{-39}\sqrt{\pi}\,\sigma}\exp\left[-\left\{\frac{\tilde{\nu}-\tilde{\nu}_i}{\sigma}\right\}^2\right]\right), \qquad (2)$$

where *i* counts the electronic excitations, R_i is the corresponding rotational strength and $\tilde{\nu}_i$ is the transition wavenumber (nm^{-1}).

Table 1 Oscillator strength (f) and rotational strength (R) of electronic transition in dimer at angles 10 ° - 80 ° in helical and creeper-helical geometry

Right-handed helix (dimer): TD-DFT calculations						
Angle	Simple-helical geometry			Creeper-helical geometry		
	Trans. Energy eV	f	R ($\times 10^{-54}$) $C^2m^3s^{-1}$	Trans. Energy eV	f	R ($\times 10^{-54}$) $C^2m^3s^{-1}$
10°	3.93	0.03	359.85	3.93	3.85	-185.02
	3.99	3.66	-358.05	3.98	0.03	174.31
20°	3.93	0.11	708.77	3.93	3.76	-363.23
	3.99	3.58	-705.24	3.97	0.11	345.07
30°	3.93	0.25	1036.18	3.94	3.61	-528.50
	3.98	3.45	-1030.86	3.97	0.25	506.59
40°	3.93	0.43	1331.98	3.94	3.41	-675.78
	3.98	3.26	-1325.33	3.97	0.43	654.04
50°	3.94	0.66	1586.88	3.94	3.16	-801.50
	3.98	3.04	-1579.81	3.97	0.67	782.23
60°	3.94	0.93	1793.22	3.95	2.89	-901.09
	3.97	2.78	-1786.53	3.96	0.94	898.72
70°	3.95	1.22	1944.50	3.95	2.58	-968.97
	3.97	2.49	-1939.47	3.96	1.24	958.57
80°	3.95	1.53	2036.46	3.95	2.25	-980.73
	3.96	2.18	-2033.70	3.96	1.57	974.88

TD-DFT results in Fig. 3 A,C,G,E demonstrate that the absolute sign of CD spectra in the long wavelength region is positive for right-handed in helix and left-handed in creeper. These results clearly indicate that the chirality rule holds for aggregates with repulsive interactions (helix), however, fails for aggregates with attractive interactions (creeper).

The intensity of calculated CD signals increases from 10° to 40°, then it decreases and vanish at 90°, wherein the system becomes achiral. The sizable rotational strengths calculated in the θ =50°- 80° range are indeed associated to weak CD signals (Fig. 4 and S2) due to the mutual cancellation of positive and negative CD signals from two states coming very close in energy.

For a quantitative comparison of TD-DFT results with the exciton model, we estimated the electrostatic interaction between the transition dipole moments using Equation 3,

$$V = \frac{1}{4\pi\varepsilon_o n^2}\left(\frac{\vec{\mu}_A \cdot \vec{\mu}_B}{r^3} - 3\frac{(\vec{\mu}_A \cdot \vec{r})\ (\vec{\mu}_B \cdot \vec{r})}{r^5}\right), \qquad (3)$$

where ε_0 is the vacuum permittivity, n is the medium refractive index and $\vec{r}$ is the vector that connects the two molecular centres. Finally, $\vec{\mu}_{A/B}$ is the transition dipole moment for the two molecules, which is set to the value calculated in TD-DFT for the isolated **PE** molecule.[14] We fix the squared refractive index (n^2) as to reproduce the exciton splitting calculated in TD-DFT for the aligned dimer. The resulting values (2.48 and 2.31 for helix and creeper, respectively) are in line with typical values for organic materials.[16] Results of the exciton model in Fig. 3 B,D,F,H confirm that the chirality rule as commonly defined only applies to chiral aggregates with repulsive interactions and cannot be generalized. We further investigated the CD response of a trimeric assembly in helical and creeper geometry (Fig. S4 and Table S2, S3). These results are again in line with the previous discussions, proving that the exciton model is fully consistent with TD-DFT results.

Having validated the exciton model against TD-DFT results for small aggregates, we exploit the exciton model to study the chiroptical response of larger aggregates. Fig. 4 reports the results for an aggregate constituted by ten molecules arranged in helix and creeper structures using same geometrical parameters as defined for the dimer. Once again, the exciton chirality rule is obeyed in the helix geometry and is broken in the creeper geometry. Of course, when ten molecules are put together, the exciton model predicts ten excited states. Nevertheless, Fig. 4 confirm that only two transitions mainly contribute to the CD spectrum, while the remaining transitions have negligible rotational strengths. In the helical geometry, the main contribution to the CD spectra is associated with states lying at higher energies (shorter wavelength). In contrast, states lying at lower energies (longer wavelength) are the dominant contributors for the creeper geometry. Thus, for a supramolecular assembly even if there are 'n' number of molecules and consequently 'n' number of higher energy states, the CD spectrum gives only a single CD couplet (provided there is single transition dipole moment, and exciton coupling is possible). We repeated the calculations for different twist angles like 45°, and 80°; the results are consistent, and the

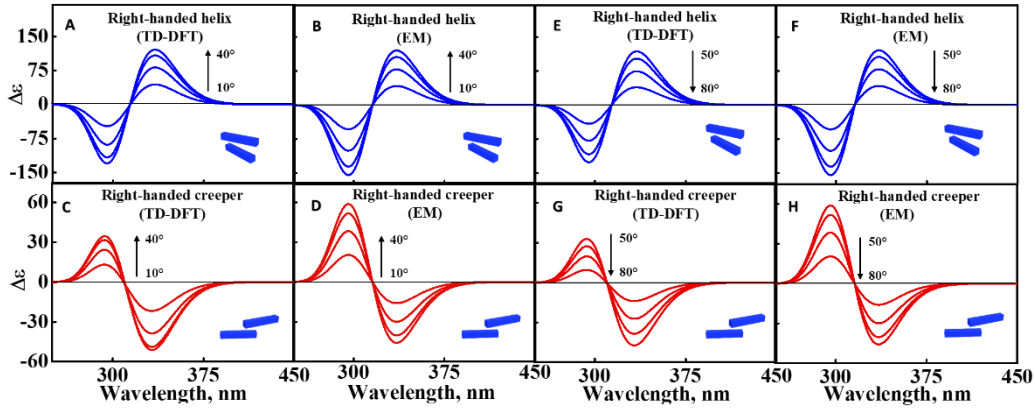

Figure 3 Calculated CD spectra of the right-handed dimer with repulsive (A,B,E,F) and attractive interactions (C,D,G,H). Spectra are shown for twist angle varying from 10° - 40° (A-D) and 50° - 80° (E-H) in 10° increment. Panels (A,C) and (E,G) show TD-DFT while panels (B,D) and (F,H) show exciton model results, respectively. Results for left-handed systems are provided in ESI (Fig. S1 and S2).

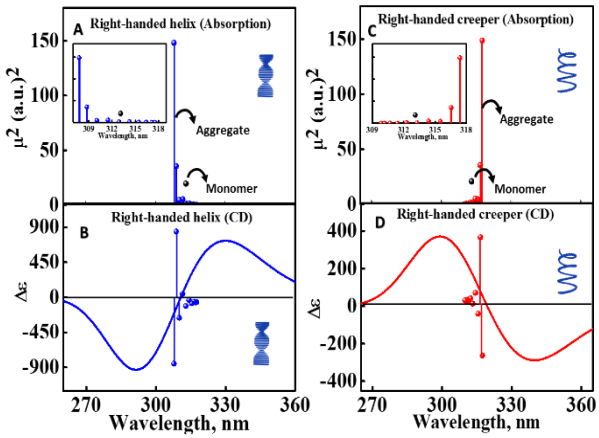

Figure 4 Exciton model calculations for a molecular aggregate of ten molecules (twist angle: 10°). Top panels (A,C): squared transition dipole moment of the monomer (black sphere) and the molecular aggregate (blue for helix and red for creeper). Insets show the same data in a zoomed scale. Bottom panels (B,D): CD spectrum of the molecular aggregate. Rotational strengths are shown as spheres (blue for helix and red for creeper) for each individual transition on the aggregate. Left panels (A,B) and right panels (C,D) refer to right-handed helix and creeper respectively.

corresponding figures are provided (Fig. S5). Moreover, change in the sign of the bisignated CD spectrum (also referred as the crossover point) of a chiral aggregate is observed in the spectral region where the absorption of the aggregate is maximum, i.e., to the blue (shorter wavelength) and to the red (longer wavelength) of the monomer absorption band for the helix and creeper, respectively.

From the above studies, it is well established that in supramolecular chiral aggregates, the sign of the CD couplet depends not only on the handedness of the aggregate, but also on the sign of the interaction energy between neighbouring dipoles. The exciton chirality rule does not account for the sign of interactions and is valid only for aggregates in which adjacent dipoles have repulsive interaction energy. Hence, when assigning the handedness of a chiral assembly based on the sign of the CD couplet, care should be given to understand the nature of interaction energy before employing the exciton chirality rule. It can be seen in the literature that incorrect reports on the absolute configuration of chiral molecules, particularly for natural products, has led to the wrong interpretation of chiral signature, which was later corrected.[17] The results presented herein provide more insight into the widely used exciton chirality method by reminding the scientific community that the interaction energy of the supramolecular assembly must also be considered while using the exciton chirality rule. The generalizations on the handedness of chiral supramolecular aggregates reported here based on the sign of CD spectra is indeed valuable for researchers working in the broad areas of chemistry and biology.

The Indo–Italian Executive Program 2017–2019 of Cooperation in Scientific & Technological Cooperation (No. INT/Italy/P-9/2016(ER)) and the dual Ph.D. degree program (S.K.) between IISER-TVM and University of Parma are acknowledged for supporting personnel exchange. Work supported by CINECA (project IscrC_CANTA) and by HPC (High Performance Computing) facility of the University of Parma, Italy. C.S. and A.P. acknowledge support from COMP-HUB Initiative, 'Departments of Excellence' program of the Italian Ministry for Education, University and Research (MIUR, 2018-2022). K.G.T. acknowledges the Department of Science and Technology (DST Nanomission Project No. SR/NM/NS-23/2016), Government of India, for financial support. This research was partly supported by the European Union Horizon 2020 programme under grant agreement No 812872 (TADFlife).

Conflicts of interest

"There are no conflicts to declare".

1 L. D. Barron, Molecular Light Scattering and Optical Activity, Cambridge University Press, Cambridge, 2 edn., 2004; A. M. Glazer and K. Stadnicka, *J. Appl. Cryst.*, 1986, **19**, 108-122.
2 H. V. P. Thelu, S. Atchimnaidu, D. Perumal, K. S. Harikrishnan, S. Vijayan and R. Varghese, *ACS Appl. Bio Mater.*, 2019, **2**, 5227-5234.
3 F. Rodríguez-Llansola, J. F. Miravet and B. Escuder, *Chem. Commun.*, 2009, DOI: 10.1039/B916250J, 7303-7305.
4 T. Verbiest, S. V. Elshocht, M. Kauranen, L. Hellemans, J. Snauwaert, C. Nuckolls, T. J. Katz and A. Persoons, *Science*, 1998, **282**, 913-915.
5 T. Noguchi, B. Roy, D. Yoshihara, J. Sakamoto, T. Yamamoto and S. Shinkai, *Angew. Chem. Int. Ed. Engl*,, 2017, **56**, 12518-12522.
6 R. Thomas, J. Kumar, J. George, M. Shanthil, G. N. Naidu, R. S. Swathi and K. G. Thomas, *J. Phys. Chem. Lett.*, 2018, **9**, 919-932.
7 N. Harada, K. Nakanishi and N. Berova, in Comprehensive Chiroptical Spectroscopy, eds. N. Berova, P. L. Polavarapu, K. Nakanishi and R. W. Woody, 2012, DOI: 10.1002/9781118120392.ch4, pp. 115-166; N. Harada, S.-M. L. Chen and K. Nakanishi, *J. Am. Chem. Soc*., 1975, **97**, 5345-5352; N. Harada and K. Nakanishi, *J. Am. Chem. Soc*., 1968, **90**, 7351-7352.
8 D. P. Craig and T. Thirunamachandran, Molecular quantum electrodynamics: an introduction to radiation-molecule interactions, Courier Corporation, 1998.
9 J. D. Chisholm, J. Golik, B. Krishnan, J. A. Matson and D. L. Van Vranken, *J. Am. Chem. Soc.*, 1999, **121**, 3801-3802; D. Gargiulo, F. Derguini, N. Berova, K. Nakanishi and N. Harada, *J. Am. Chem. Soc.*, 1991, **113**, 7046-7047; S. Matile, N. Berova, K. Nakanishi, J. Fleischhauer and R. W. Woody, *J. Am. Chem. Soc.*, 1996, **118**, 5198-5206.
10 T. Bruhn, G. Pescitelli, S. Jurinovich, A. Schaumlöffel, F. Witterauf, J. Ahrens, M. Bröring and G. Bringmann, *Angew. Chem. Int. Ed. Engl*,, 2014, **53**, 14592-14595; S. Jurinovich, C. A. Guido, T. Bruhn, G. Pescitelli and B. Mennucci, *Chem. Commun.*, 2015, **51**, 10498-10501.
11 S. Abbate, G. Mazzeo, S. Meneghini, G. Longhi, S. E. Boiadjiev and D. A. Lightner, *J. Phys. Chem. A*, 2015, **119**, 4261-4267.
12 E. U. Condon, *Rev. Mod. Phys.*, 1937, **9**, 432-457.
13 M. Anzola, F. Di Maiolo and A. Painelli, *Phys. Chem. Chem. Phys.*, 2019, **21**, 19816-19824.
14 S. Kar, K. Swathi, C. Sissa, A. Painelli and K. G. Thomas, *J. Phys. Chem. Lett.*, 2018, **9**, 4584-4590.
15 P. J. Stephens and N. Harada, *Chirality*, 2010, **22**, 229-233.
16 D. Bialas, C. Zhong, F. Würthner and F. C. Spano, *J. Phys. Chem. C*, 2019, **123**, 18654-18664.
17 C. L. Covington, V. P. Nicu and P. L. Polavarapu, *J. Phys. Chem. A*, 2015, **119**, 10589-10601; M. Enamullah, G. Makhloufi, R. Ahmed, B. A. Joy, M. A. Islam, D. Padula, H. Hunter, G. Pescitelli and C. Janiak, *Inorg. Chem.*, 2016, **55**, 6449-6464.